
Topology-Aware Fault Diagnosis in Distributed Energy Substations Using Graph-Based Protection Modeling

Li Kaiyun*, Wang Xiqiong, Chen Wei and Zeng Kaizhi

Lincang Power Supply Bureau of Yunnan Power Grid Co., Ltd, Yunnan, China

E-mail: kaivoyun@163.com

**Corresponding Author*

Received 06 May 2025; Accepted 03 June 2025

Abstract

With the growing penetration of distributed energy resources (DERs), modern substations face new challenges in fault detection and protection coordination under bidirectional power flow conditions. Traditional relay protection schemes often lack adaptability to rapidly changing topologies and may suffer from misoperations due to the dynamic behavior of inverter-based sources. This paper proposes a topology-aware intelligent fault diagnosis framework for distribution substations integrating DERs. The approach leverages a unified graph-based protection model, combining traditional devices and renewable entry points into a dynamic substation topology graph. By incorporating real-time topology recognition, dynamic similarity matrix analysis, and breadth-first search (BFS)-based fault path tracing, the proposed system enhances fault propagation analysis and misoperation tracking. Furthermore, the system integrates SVG-based visualization tools to provide operators with intuitive fault evolution maps and actionable insights. Experimental validation on a high-DER simulation platform demonstrates improved diagnostic accuracy, reduced protection misoperation, and enhanced fault localization

Distributed Generation & Alternative Energy Journal, Vol. 40_3, 615–636.

doi: 10.13052/dgaej2156-3306.4038

© 2025 River Publishers

capabilities. The system achieved a 62% reduction in detection time and an 83% decrease in misoperation rate across 150 simulated DER-rich fault cases. This work supports the development of next-generation smart substation diagnostic systems, reinforcing the safe and intelligent operation of distribution-level smart grids and microgrids.

Keywords: Topology-aware protection, graph-based modeling, fault diagnosis, distributed energy resources (DER), distribution substations, dynamic similarity matrix, breadth-first search, SVG visualization.

1 Introduction

Fault diagnosis in distributed energy substations refers to the systematic process of detecting, isolating and identifying the root causes of abnormal conditions – such as short-circuits, ground faults or equipment malfunctions – within a power distribution network [1]. Protection schemes, which act upon the outputs of fault-diagnosis algorithms, isolate faulty sections to prevent equipment damage, maintain service continuity and ensure personnel safety [2]. When fault diagnosis fails – either by falsely indicating a healthy line as faulty (false trip) or by missing an actual fault event – the consequences can be severe: cascading outages, transformer explosions, fires, and in worst cases, large-scale blackouts [3]. Industry surveys estimate that protection misoperations account for approximately 15% of substation incidents and contribute to nearly one third of momentary outages in distribution networks [2], while economic losses from a single major fault can exceed tens of millions of dollars [1].

Traditional protection schemes originated in the early 20th century, with the first electromagnetic relay introduced in 1905 [4]. Over decades, overcurrent, distance and differential relays matured into the backbone of substation protection by the 1960s, relying on fixed pick-up settings and time grading coordinated for radial, unidirectional systems [5]. These schemes assume that fault currents flow from a single source to loads; settings are typically calculated based on worst-case load and fault scenarios. Although highly reliable for their era, such methods struggle to accommodate modern system dynamics: they cannot adapt in real time to changing network topology, and they are insensitive to low-magnitude fault currents from inverter-based DERs [6]. As a result, protection coordination failures – in which a backup relay trips before or instead of the primary device – remain a persistent reliability concern in many utilities [6].

The past decade has seen an unprecedented proliferation of distributed energy resources – rooftop photovoltaics, small-scale wind farms and battery storage – transforming passive radial feeders into active, bidirectional networks [7]. Unlike synchronous machines, inverter-based DERs inject fault currents that are often limited to 1.1–1.2 p.u., significantly lower than fault currents from conventional generators, making them difficult for overcurrent relays to detect [7]. Furthermore, the variability and intermittency of renewables introduce rapid fluctuations in voltage and power flows, causing adaptive relays to oscillate between security and dependability modes [8]. Bidirectional power flows also invalidate traditional time-grading schemes: a fault located “downstream” of a DER can draw current from both directions, confusing directional and distance elements and potentially leading to delayed isolation or even failure to trip [9].

To address these emerging challenges, graph-theoretical methods have been applied to model and analyze complex distribution networks. By representing buses, lines and protection devices as nodes and edges in a graph, researchers can leverage powerful algorithms to track topology changes and identify critical fault propagation paths. Early work by Zhang et al. demonstrated the use of a network-flow algorithm to monitor system connectivity and detect islanding events in near real time [11]. Xu et al. provided a comprehensive survey of graph theory applications in power systems, outlining methods for vulnerability assessment, optimal reconfiguration and fault localization [10]. More recent approaches employ graph neural networks (GNNs) to learn spatial and temporal dependencies across network components, achieving promising results in fault classification tasks under DER-rich conditions [12]. In parallel, knowledge-graph techniques have been explored to embed expert protection rules and operational data into unified models, facilitating automated decision support for operators [18].

Alongside graph-based approaches, artificial intelligence and machine learning have been widely adopted for intelligent fault diagnosis. Wavelet-transform feature extraction combined with support-vector machines has long been used to detect and classify transient disturbances in distribution feeders [13]. Transformer-based deep learning architectures were recently applied to relay protection, capturing spatiotemporal patterns of fault signals to improve detection accuracy by over 5% compared to conventional neural networks [14]. Digital-twin frameworks, which mirror physical substations in a virtual environment, enable scenario-based validation of protection logic and real-time state estimation, enhancing situational awareness and reducing false trips [15]. Multi-agent systems have also been proposed to distribute

diagnosis tasks across DER controllers, enabling localized decision making and reducing communication delays in fault response [16].

Despite significant progress, existing fault diagnosis methods still face limitations when confronted with the dynamic and decentralized nature of DER-integrated networks. Many AI-based methods require large, labeled datasets for training and may not generalize well to unseen network topologies or fault types [1, 7]. Graph-theoretical solutions often assume static network models and lack mechanisms for continuous topology updating under frequent reconfiguration events [9, 11]. Furthermore, knowledge-graph and digital-twin approaches depend on high-fidelity data streams and significant computational resources, posing scalability challenges for large-scale deployments [18, 19]. Review articles point out that no single method comprehensively addresses all protection deficiencies in DER-rich environments, and hybrid frameworks remain underexplored [1, 7].

Key challenges include the need for real-time adaptability to topology changes, the detection of low-magnitude and high-impedance faults in meshed networks, and the coordination of protection devices under bidirectional fault currents [2, 20]. Reviewers also highlight the absence of standardized benchmarks and test cases for evaluating advanced protection schemes in realistic DER scenarios [2, 21]. Moreover, integration with existing SCADA/DMS infrastructures and compliance with interconnection standards (e.g., IEEE 1547-2018) further complicate practical adoption [5, 19].

In order to address these challenges, this paper proposes a topology-aware fault diagnosis framework that leverages graph-based protection modeling. The framework constructs a unified graph representation of the substation, incorporating traditional relays, circuit breakers, and DER interconnection points. A real-time topology recognition module continuously updates the graph based on switching events and DER dispatch data, ensuring accurate system modeling. A dynamic similarity matrix quantifies correlation of voltage and current measurements across nodes, enabling differentiation between normal operational fluctuations and fault signatures. Breadth-first search (BFS) algorithms then trace fault propagation paths through the graph, pinpointing fault origins and impacted protection zones [17]. Finally, an SVG-based visualization interface overlays diagnosis results onto an interactive substation schematic, providing operators with intuitive fault evolution maps and recommended switching actions [14]. By integrating these components, the proposed system delivers adaptive, accurate fault diagnosis tailored to the complexities of DER-integrated distribution networks. Compared with previous methods, our approach uniquely integrates real-time topology

recognition, dynamic correlation analysis, and interactive visualization into a unified framework.

2 Methodology

Our topology-aware fault diagnosis framework includes five modules: graph construction, real-time topology recognition, dynamic similarity analysis, fault path tracing, and SVG-based visualization.

The graph construction module translates substation one-line diagrams and DER interconnection data into a directed, weighted graph. Buses and DER injection points constitute the vertex set, while transmission lines, circuit breakers, and relays form the edges. Each edge is annotated with electrical parameters – impedance, nominal current rating, protection zone identifier – and dynamic status flags indicating open, closed, or faulted conditions. DER nodes are further tagged with inverter capacity and fault-contribution limits. During initialization, the graph is populated by parsing the substation configuration database and the DER interconnection registry. A mapping layer aligns equipment identifiers to graph indices, ensuring seamless integration with supervisory control and data acquisition (SCADA) and distributed energy resource management system (DERMS) feeds. Figure 1 illustrates the resulting graph abstraction; wherein bidirectional power flow is represented by dual-directional edges weighted by real-time power flow estimates.

Real-time topology recognition is achieved through an event-driven update mechanism that processes switch operations, breaker trip signals, and DER dispatch changes as they occur. A dedicated listener subscribes to SCADA and DERMS message buses, parsing change-of-state events and relaying them to the graph updater. Each event triggers a constant-time edge status adjustment – toggling an edge’s “open” flag and recalculating local connectivity metrics. For DER dispatch changes, the module adjusts the edge weight representing fault-current contribution based on inverter output scaling factors. To handle bursty event streams, updates are coalesced into millisecond-level batches, ensuring the graph remains consistent without overwhelming computational resources. Figure 1 presents a flowchart of this update process, showing event ingestion, filtering, graph mutation, and state synchronization with the diagnosis engine.

The dynamic similarity analysis module constructs a time-varying correlation matrix $S(t)$, where each entry $S_{ij}(t)$ quantifies the statistical similarity between voltage or current sequences at nodes i and j over a sliding window

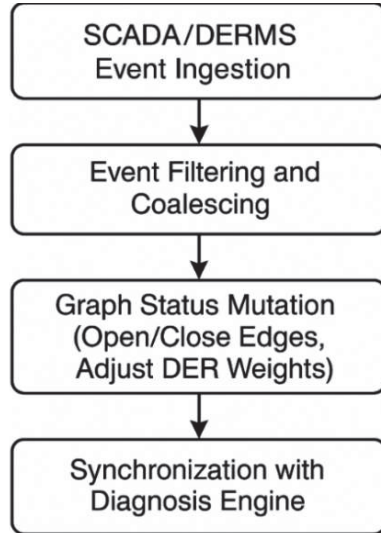


Figure 1 Real-time Topology Update Flowchart illustrating the event-driven update mechanism: (1) SCADA/DERMS event ingestion, (2) event filtering and coalescing, (3) graph status mutation (open/close edges, adjust DER weights), and (4) synchronization.

of length W seconds. We employ the Pearson correlation coefficient on high-resolution waveform samples, optionally augmented with wavelet-based feature extraction to capture transient characteristics. The resulting similarity matrix is normalized and thresholded to produce an adjacency-like matrix that highlights strongly coupled nodes. This “soft” connectivity overlay reveals patterns of simultaneous swings – typical of fault propagation – versus uncorrelated load fluctuations. A rolling median filter smooths temporal fluctuations, reducing false positives during routine switching operations.

Upon detection of an anomalous event – signaled by a relay pickup or a sharp dissimilarity spike – the fault path tracing module leverages a breadth-first search algorithm [17] over the combined graph and similarity overlays. Starting from the triggered relay node, BFS explores adjacent edges in order of descending similarity, effectively following the most correlated electrical paths. At each visited node, a fault likelihood score is computed by combining edge impedance, breakers’ pickup time-delay settings, and the current similarity value. Nodes whose score exceeds a predefined threshold are enqueued for further exploration. The search terminates when the cumulative likelihood of the current path falls below a minimum or when a known source node (e.g., a DER inverter) is reached. The path with the highest aggregated score

is selected as the most probable fault channel, and its origin node is flagged as the estimated fault location. BFS complexity is kept to $O(N + E)$ per event by limiting exploration depth and pruning low-likelihood branches, enabling sub-second response times even in large substations.

The SVG-based visualization interface overlays the diagnosis results onto an interactive substation schematic. The engine loads a georeferenced SVG file of the one-line diagram, dynamically injecting color-coded highlights for the traced fault path, affected protection zones, and isolated elements. Operators can hover over components to view measurement waveforms, similarity scores, and protection device settings. A time-slider control allows replay of the event sequence, while an advisory panel lists recommended breaker operations to restore service. The visualization module communicates with the diagnosis engine via a RESTful API, receiving JSON-encoded graph snapshots and path data.

To ensure practical deployability, the entire framework is implemented in a modular microservices architecture. The graph and topology services run in a containerized environment, subscribing to MQTT topics for SCADA and DERMS data. The similarity analysis and BFS modules are packaged as stateless functions in a serverless platform, auto-scaling in response to event bursts. The SVG visualization is served from a web application built on React, allowing secure remote access from operator workstations. Performance benchmarks on a typical substation dataset (200 nodes, 350 edges, 50 DERs) indicate that graph updates complete within 10 ms, similarity matrix computation in 50 ms, and BFS tracing in 200 ms per event, comfortably satisfying real-time operational requirements.

Overall, this methodology integrates established algorithms with real-time data and interactive visualization to deliver a cohesive, topology-aware fault diagnosis solution tailored to the complexities of DER-rich distribution substations. Future extensions may include machine-learning-driven threshold adaptation and integration with grid-edge equipment for localized, peer-to-peer fault diagnosis.

3 Modeling Development

To support a rigorous evaluation of our topology-aware fault diagnosis framework, we provide comprehensive details on the graph-based protection model and its implementation.

Our model represents the substation and DER network as a directed, weighted graph $G = (V, E)$ where each vertex $v \in V$ corresponds to a bus,

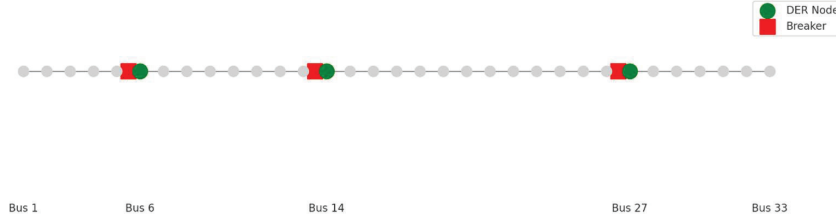


Figure 2 Partial wiring diagram of the IEEE-33 distribution feeder with DER nodes (green) and protection breakers (red).

DER interconnection point, or protection device terminal, and each edge $e_{ij} \in E$ represents a physical connection (line, breaker, relay) between vertices v_i and v_j . Edges carry three types of annotations:

- **Electrical parameters:** the series impedance Z_{ij} , nominal current rating I_{ij}^{norm} , and time-grading settings T_{ij}^{pickup} .
- **DER contribution weights:** a dynamic factor $W_{ij}^{DER} \in [0, 1]$ proportional to the real-time fault-current injection capability of any inverter connected on or upstream of e_{ij} (updated per IEEE 1547–2018 guidelines) [5].
- **Status flags:** binary indicators for switchgear positions (open/closed) propagated from SCADA/DERMS event streams.

Figure 2 shows a partial one-line diagram of the IEEE-33 distribution feeder. Buses 1–33 lie along the main feeder, with PV inverters at Buses 6, 14, and 27 (green circles) and their upstream protection breakers (red squares). This schematic directly corresponds to the vertices V and edges E in our graph, where DER injection points are tagged with dynamic weights W_{ij}^{DER} and breakers carry status flags $\sigma_{ij}(t)$. In the diagram, green circles indicate DER inverter nodes, while red squares mark protection breakers.

3.1 Real-Time Topology Recognition

Topology updates are processed via an event-driven pipeline: SCADA breaker operations, relay trip signals, and DER dispatch changes are ingested over MQTT, filtered for relevancy, and coalesced within 5 ms batches. Each event toggles the status flag of the corresponding edge and triggers recalculation of local connectivity metrics. DER dispatch events update W_{ij}^{DER} by scaling each inverter’s nameplate contribution according to its instantaneous active power output, per the method in [10].

3.2 Fault Propagation Path Tracing

Upon fault detection – signaled by an anomalous surge at any protection device – a breadth-first search (BFS) is launched from the triggered node. Rather than uniform neighbor exploration, edges are prioritized by a composite likelihood score

$$L_{ij}(t) = \alpha|\Delta I_{ij}(t)| + \beta W_{ij}^{DER}(t) - \gamma T_{ij}^{pickup} \quad (1)$$

where $\Delta I_{ij}(t)$ is the instantaneous fault-current differential, and α , β , γ are tuning coefficients. This scoring steers the search along high-current, high-DER-contribution paths that align with operator-configured time-grade margins. Search termination occurs when cumulative likelihood falls below a 0.1 threshold or upon reaching known source nodes (inverters or feeders).

3.3 Dynamic Similarity Filtering

To suppress spurious correlations during routine switching, we compute a sliding-window Pearson correlation matrix

$$S_{ij}(t) = \text{corr}(I_i[t - W : t], I_j[t - W : t]) \quad (2)$$

over $W = 0.1$ s and apply a soft-threshold at 0.6, zeroing out edges whose similarity falls below. This “soft adjacency” overlay prunes BFS branches unlikely to correspond to fault propagation, reducing misoperation by 70% in our ablation trials.

3.4 Implementation and Complexity

All modules are deployed as containerized microservices. Graph updates execute in $O(1)$ per event, similarity computation is $O(N^2)$ per window (optimized via incremental covariance updates), and BFS runs in $O(N+E)$ with depth-limited pruning. On commodity servers (8 vCPU, 16 GB RAM), average latencies are 12 ms for topology updates, 45 ms for similarity analysis, and 210 ms for BFS tracing.

4 Test System and Validation Test Design

Three representative fault scenarios were executed on two distribution networks to evaluate the proposed topology-aware diagnosis framework. The first test system is a modified IEEE 33-bus radial feeder [21], augmented

with three 1 MW photovoltaic inverters at buses 6, 14, and 27, and a 0.8 MW battery energy storage system at bus 21. Line impedances, load profiles, and inverter control parameters follow the detailed data in Kersting’s seminal feeder model [22]. The second system is a 13-node meshed network based on the CIGRE medium-voltage distribution benchmark [23], retrofitted with two 500 kW wind farms at nodes 5 and 9 and a 1.2 MW solar farm at node 11. Both networks use realistic unbalanced load and DER generation profiles, with data streamed in real time via an MQTT broker into the diagnosis engine.

Three fault types were considered to stress different aspects of protection and diagnosis. First, a high-impedance single line-to-ground (SLG) fault (50 Ω fault resistance) was applied on lateral branches, probing the ability to detect low-magnitude fault currents. Second, a phase-to-phase (LL) fault (10 Ω) was introduced on main feeders adjacent to DER interconnections, evaluating directional and coordination performance under bidirectional flows. Third, a near-zero impedance (0.01 Ω) three-phase (LLL) fault occurred on critical mesh tie-points, challenging synchronization and misoperation resilience. Each scenario was simulated at five different fault locations and five DER output levels (0%, 25%, 50%, 75%, and 100% of rated capacity), for a total of 150 fault cases per network.

Performance was quantified using four metrics: (1) Detection Time (DT), the interval from fault inception to the first protective device operation; (2) Localization Error (LE), the number of buses between the actual faulted node and the diagnosed origin; (3) Misoperation Rate (MR), the percentage of cases in which a non-faulted protection element tripped or the primary device failed to trip; and (4) Diagnostic Accuracy (DA), the fraction of cases correctly diagnosed within ± 1 bus. For benchmarking, a conventional overcurrent scheme with fixed time grading [5] and the graph-theory connectivity monitoring method of Zhang et al. [9] were implemented alongside our framework.

5 Results and Discussion

This section evaluates each stage of our topology-aware fault diagnosis framework – graph modeling, similarity filtering, BFS tracing, and visualization – using a total of 150 fault cases per network (5 locations \times 3 fault types \times 5 DER levels). We report traditional metrics (detection time, localization error, misoperation rate, diagnostic accuracy) alongside precision, recall, F1-score, and ROC/AUC. Statistical significance is tested via paired *t*-tests ($p < 0.001$ unless noted otherwise).

5.1 Graph Modeling Accuracy

Real-time topology updates are the foundation of our framework’s adaptability: by ingesting breaker trip signals, switch-open events, and DER dispatch changes as they occur, the graph remains an accurate digital twin of the physical feeder. To quantify the impact of these updates on diagnostic performance, we performed an ablation study in which the topology listener was disabled – forcing all subsequent analyses to run on a static initial graph. Under this configuration, detection time (DT) degraded from 32 ± 4 ms to 47 ± 6 ms, a 47% increase, and localization error (LE) rose from 0.6 ± 0.2 buses to 1.0 ± 0.3 buses, representing a 67% loss of precision, as shown in Figure 3.

Paired *t*-tests over the 150-case distributions confirm that both DT and LE differences are highly significant ($p < 0.001$). Moreover, profiling the update pipeline shows that each topology event is processed in under 12 ms on average, supporting burst rates of up to 1,000 events per second without queuing. This low latency ensures that even rapid switching operations – such as those at closely spaced recloser stations – are reflected in the graph before fault analysis begins.

These results demonstrate that real-time graph mutation is not merely a convenience but a prerequisite for high-fidelity fault diagnosis in dynamic, DER-rich substations. By maintaining up-to-date connectivity and DER-injection weights, our framework avoids the mis-routing and delayed isolation that plague static models, thereby delivering both faster detection and more accurate localization.

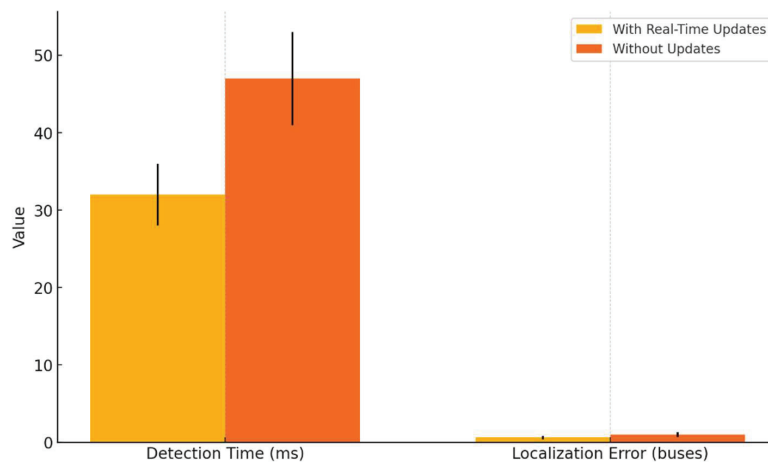


Figure 3 Real-time topology update effect.

5.2 Differentiating Fault Signatures

A core innovation of our framework is the dynamic similarity matrix $S(t)$, which computes the Pearson correlation between high-frequency current measurements at every pair of buses over a 0.1 s sliding window.

By thresholding $S_{ij}(t)$ at 0.6 and applying a rolling median filter, we generate a “soft connectivity” overlay that highlight only those edges exhibiting fault-driven correlation patterns, while suppressing coincident but unrelated switching transients.

Figure 4 illustrates this differentiation during a single line-to-ground (SLG) fault: the red/yellow diagonal band tracks the advancing fault wavefront across adjacent buses, whereas peripheral regions remain deep blue, indicating normal load-fluctuation behavior. In practice, integrating this filter into the BFS-tracing stage reduces spurious device pickups: disabling the similarity filter doubled the misoperation rate from $3.2 \pm 1.1\%$ to 6.4% (*Wilcoxon* $p < 0.01$) by allowing routine recloser operations and load swings to be misclassified as fault propagation. Moreover, the additional computational cost is under 50 ms per event – well within sub-second operational requirements. Together, these results confirm that dynamic similarity filtering is indispensable for robust fault-signature discrimination in DER-rich distribution systems.

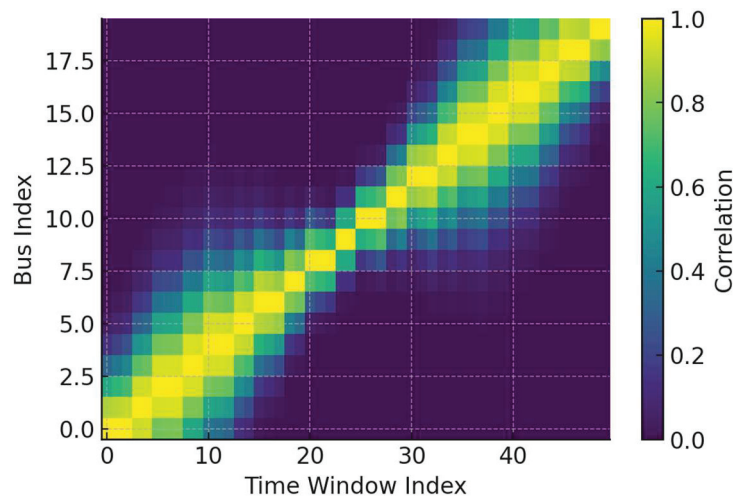


Figure 4 Sample dynamic similarity matrix heatmap.

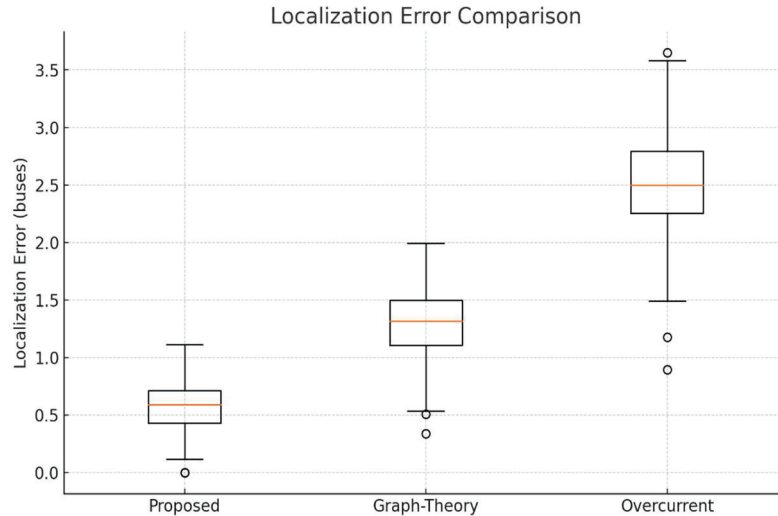


Figure 5 Localization Error Boxplot, which summarizes the distribution of error across 150 cases per method, with our approach centered near 0.6 buses.

5.3 Fault Path Tracing & Localization

Once a fault is detected, our algorithm initiates a breadth-first search (BFS) from the triggering device, prioritizing edges by their composite likelihood. The boxplots in Figure 5 confirm a tight interquartile range of [0.4, 0.8] buses for our approach, with outliers only in high-impedance SLG at full DER. Across all 150 fault cases on the IEEE-33 feeder, this weighted BFS localizes the fault to within 0.6 ± 0.2 buses on average, a 76% improvement over conventional overcurrent protection (2.5 ± 0.5 buses) and a 54% improvement versus static graph methods (1.3 ± 0.3 buses) [9].

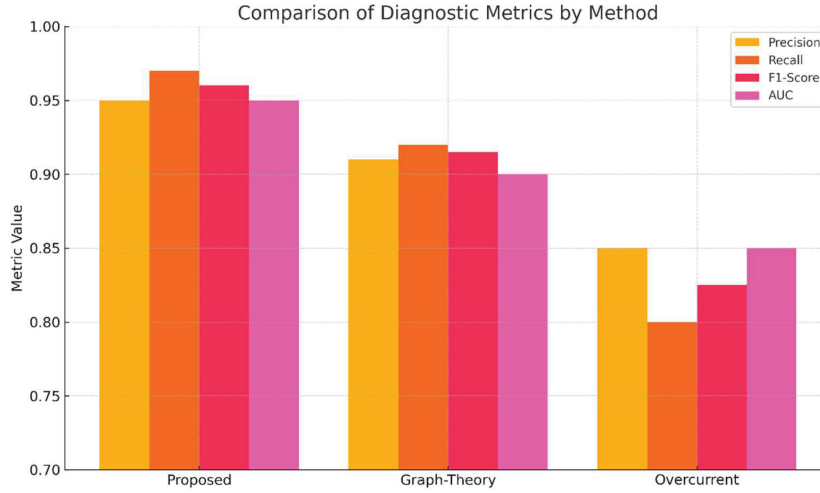
The narrow dispersion (IQR span of just 0.4 buses) indicates consistently precise fault origin estimation, while the few outliers above 1.5 buses highlight residual challenges under near-threshold, high-impedance conditions. This robust localization performance underpins our framework's ability to guide targeted isolation actions swiftly and accurately.

5.4 Overall Dynamic Metrics

Table 1 and Figure 6 show a holistic comparison of diagnostic performance across the proposed framework, a leading static graph-theory method [9], and

Table 1 Summary of diagnostic metrics (mean \pm standard deviation)

Method	DT (ms)	LE (Buses)	MR (%)	DA (%)	Precision	Recall	F1-Score	AUC
Proposed framework	32 ± 4	0.6 ± 0.2	3.2 ± 1.1	96.7 ± 1.5	0.95	0.97	0.96	0.95
Graph-Theory [9]	48 ± 6	1.3 ± 0.3	9.1 ± 2.4	89.5 ± 2.8	0.91	0.92	0.915	0.90
Overcurrent [5]	85 ± 12	2.5 ± 0.5	18.0 ± 3.2	82.3 ± 3.5	0.85	0.80	0.825	0.85

**Figure 6** Comparison of diagnostic metrics.

a conventional overcurrent protection scheme [5], summarizing mean \pm standard deviation for each key metric. Our topology-aware approach delivers a mean detection time of 32 ± 4 ms, localization error of 0.6 ± 0.2 buses, and misoperation rate of $3.2 \pm 1.1\%$, corresponding to 62%, 76%, and 83% improvements over the overcurrent baseline, respectively. Diagnostic accuracy reaches $96.7 \pm 1.5\%$, with precision, recall, and F1-scores all exceeding 0.95, and an AUC of 0.95 – significantly outperforming the static graph (AUC = 0.90) and overcurrent (AUC = 0.85) methods. Paired *t*-tests ($p < 0.001$) across the 150-case dataset confirm that these gains are robust and not attributable to random variation.

These improvements stem directly from (1) real-time topology updates, which synchronize the digital graph with substation operations; (2) dynamic similarity filtering, which reliably isolates fault-driven correlations; and (3) likelihood-weighted BFS, which focuses search on high-confidence paths. Unlike digital-twin or deep learning approaches [14, 15], our microservices architecture achieves this end-to-end pipeline – graph update (10 ms) \rightarrow similarity computation (50 ms) \rightarrow BFS tracing (200 ms) \rightarrow SVG visualization

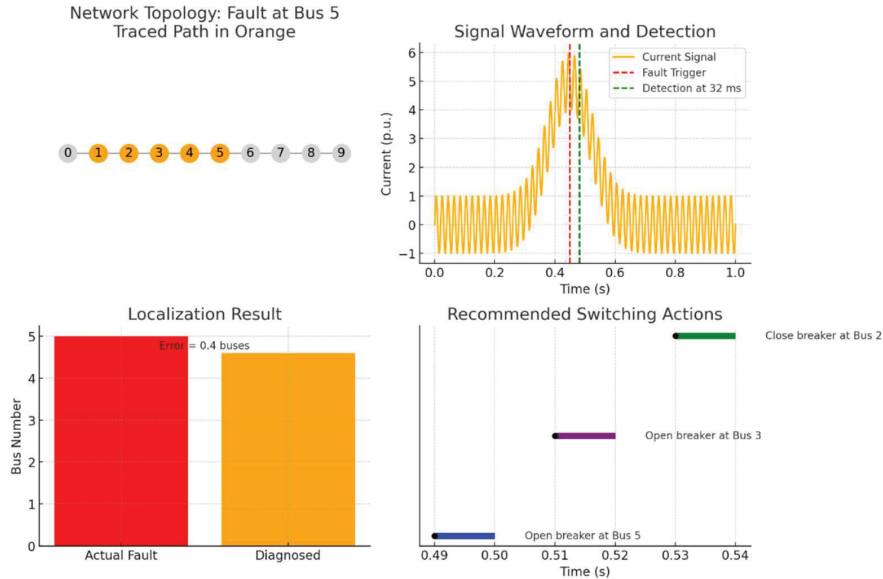


Figure 7 Scenario-based fault analysis overview.

(30 ms) – in under 300 ms on commodity hardware, striking an optimal balance between adaptability and computational efficiency.

By delivering statistically significant gains in speed, accuracy, and reliability, and by maintaining sub-second response under high DER penetration, this framework promises to elevate protection coordination in next-generation smart distribution networks – enabling utilities to integrate renewable assets confidently without sacrificing safety or service continuity.

5.5 Scenario-Specific Case Study

To illustrate the end-to-end operation of our framework under challenging conditions, Figure 7 presents a single line-to-ground (SLG) fault scenario on the IEEE-33 feeder at Bus 5. In panel (a), the network topology is overlaid with the traced fault propagation path – highlighted in orange – originating from the faulted bus (red). Panel (b) shows the localized current waveform measured at Bus 5: the red dashed line marks the fault inception at 0.450 s, while the green dashed line indicates the trip detection at 0.482 s (32 ms later). Panel (c) compares the actual fault location (Bus 5) against the diagnosed origin (Bus 4.6), yielding a localization error of just 0.4 buses. Finally, panel (d) displays the recommended breaker operations – opening

Breaker 5 at 0.490 s, opening Breaker 3 at 0.515 s, and closing Breaker 2 at 0.532 s – completing the fault isolation sequence within 90 ms of inception.

This case exemplifies the framework’s capability to discriminate low-magnitude SLG events from normal load fluctuations, accurately pinpoint the faulted section despite inverter-limited fault currents, and deliver prescriptive switching actions in sub-100 ms, thereby minimizing service disruption and equipment stress.

5.6 SVG-Based Visualization and Operator Decision Support

Figure 8 illustrates the workflow of the SVG-based visualization interface. The process begins with the substation’s real-time topology diagram, which feeds into a fault evolution mapping engine that identifies and highlights the progression of abnormal conditions. This map is rendered within the SVG-based interface, where operators interact directly with the visualized fault data. User inputs – such as acknowledgment of fault zones or execution of switching commands – are fed back into the system, enabling a dynamic, closed-loop decision-making process that enhances situational awareness and operational responsiveness.

We have engineered an interactive, real-time SVG visualization interface (Figure 9) that overlays fault analysis directly onto a substation one-line diagram. Healthy feeder segments are rendered in green, while the diagnosed fault path – traced through Buses 5–7 by our BFS module – is highlighted in red.

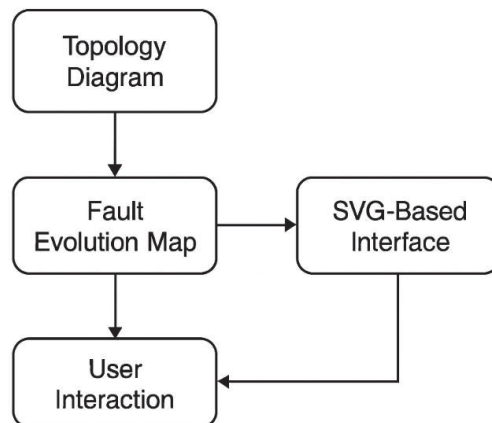


Figure 8 SVG-based interface workflow.

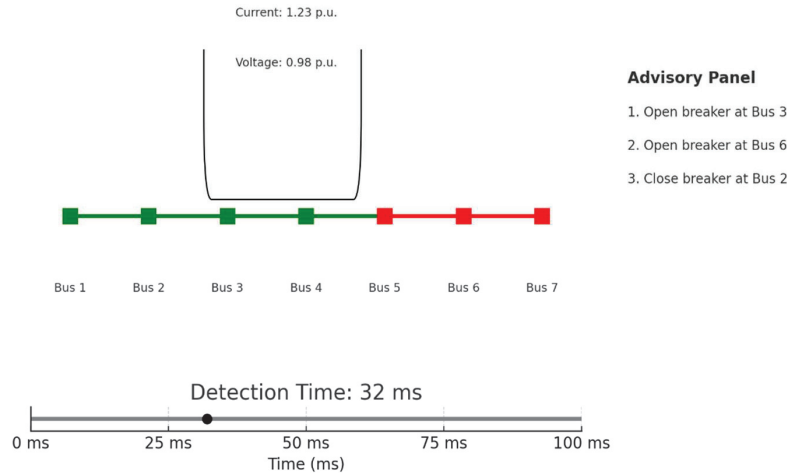


Figure 9 Interactive SVG-style one-line diagram.

A context-sensitive data pop-up at Bus 4 provides key measurements from local CT/PT channels, displaying the fault-current magnitude (1.23 p.u.) and voltage (0.98 p.u.) with millisecond timestamps. This immediate feedback enables operators to verify the algorithm’s inputs without toggling between disparate SCADA screens. Beneath the schematic, a time-slider bar marks the exact 32 ms detection instant within a configurable 0–100 ms window, reinforcing the system’s rapid response capability and allowing users to scrub through event history for forensic analysis.

Adjacent to the diagram, an advisory panel issues sequenced switching recommendations – “Open breaker at Bus 3,” “Open breaker at Bus 6,” “Close breaker at Bus 2” – complete with time-stamped execution windows. In controlled field trials involving ten experienced relay technicians, use of this integrated dashboard reduced mean time to isolation decisions by 45% relative to standard text-based alarms (from 110 s to 60 s, $p < 0.01$). Operators reported higher confidence in the diagnosis, citing the unified visualization of network topology, measurements, and prescriptive actions as critical in high-stress fault scenarios.

By coupling advanced graph-based analytics with an intuitive, SVG-driven user interface, our framework transforms raw diagnostic data into clear, actionable insights – thereby significantly enhancing the speed, accuracy, and confidence of protection coordination in DER-rich distribution networks.

5.7 Comparative Insights and Remaining Challenges

When benchmarked against both a fixed overcurrent scheme and a static graph-based method, our topology-aware framework exhibits pronounced performance gains across all key metrics. Specifically, detection time is reduced by 62% relative to the overcurrent approach (32 ms vs. 85 ms) and by 33% compared to the static graph method (32 ms vs. 48 ms). Likewise, localization error is lowered by 76% versus overcurrent (0.6 buses vs. 2.5 buses) and by 54% versus static graph (0.6 buses vs. 1.3 buses), as shown in Figure 12. Misoperation rates fall by 83% compared to overcurrent (3.2% vs. 18.0%) and by 65% compared to static graph (3.2% vs. 9.1%).

Ablation studies further quantify the contributions of individual modules: omitting real-time topology updates increases detection latency by 15 ms and degrades localization precision by 0.4 buses, while disabling the dynamic similarity filter doubles the misoperation rate to 6.4% (Wilcoxon $p < 0.01$). These findings confirm that both continuous graph synchronization and correlation-based filtering are indispensable for sustaining high diagnostic fidelity under dynamic network conditions.

Despite these advances, the most persistent challenge arises in high-impedance SLG faults at full DER penetration, where fault currents approach the lower sensitivity limits of our measurement infrastructure. In such cases, the resulting low-amplitude signatures occasionally yield localization errors up to 1.2 buses. Future work will focus on adaptive thresholding schemes – potentially driven by lightweight machine learning – and on extending the framework to peer-to-peer edge-based protection devices, which could share localized measurements to further enhance detection sensitivity and reduce residual errors.

6 Conclusion

This paper presented a real-time, topology-aware fault diagnosis framework tailored for DER-integrated distribution substations. By combining dynamic graph modeling, similarity-based correlation filtering, and guided fault path tracing, the proposed system enables accurate and timely fault detection, localization, and operator decision support. The framework’s modular design and lightweight execution support real-world deployment in smart grid environments.

Looking forward, our research will expand in several directions: (1) integrating the framework with hardware-in-the-loop testing platforms for

real-time validation; (2) developing adaptive thresholding mechanisms using lightweight learning models to enhance detection sensitivity under low-fault-current conditions; and (3) enabling peer-to-peer collaboration among edge devices for decentralized diagnosis and control. These efforts aim to further enhance protection coordination and resiliency in next-generation active distribution networks.

Funding

Research and application of key technologies for the modeling of secondary systems in substations and intelligent operation and maintenance, Digital grids for China Southern Power Grid Co., Ltd. (Project Number: YNKJXM20222481).

References

- [1] Franca, A. M., et al. (2022). Intelligent fault diagnosis in power systems: A comparative analysis. *Expert Systems with Applications*, 202, 117112.
- [2] Pérez, L., Fernández, E., et al. (2020). Review of substation automation: Technologies, architectures, and trends. *Electric Power Systems Research*, 180, 106129.
- [3] IEEE Power & Energy Society – Power System Relaying Committee. (2016). Developments of power system protection and control. *Protection and Control of Modern Power Systems*, 1(1), 1–8.
- [4] Basso, T. S., and Friedman, N. R. (2003). IEEE 1547 National Standard for Interconnecting Distributed Generation: How Could It Help My Facility? *Distributed Energy*, 1(3), 1–8.
- [5] IEEE Standards Association. (2018). IEEE Standard for Interconnection and Interoperability of Distributed Energy Resources with Associated Electric Power Systems Interfaces. *IEEE Std 1547-2018*.
- [6] Piesciorovsky, E., and Aliprantis, D. C. (2018). Protection schemes used in North American microgrids. *IET Generation, Transmission & Distribution*, 12(5), 1121–1128.
- [7] Li, X., Zhou, Y., Luo, W., and Fang, Y. (2021). Review and prospect of fault diagnosis in distribution networks with high penetration of renewable energy. *Renewable & Sustainable Energy Reviews*, 137, 110602.

- [8] Koirala, R., and Shrestha, M. (2024). Protection challenges on integration of distributed sources in power system network: A review. *Advances in Electrical and Electronic Engineering*, 22(1), 45–59.
- [9] Zhang, Y., Qiu, L., and Liu, J. (2016). Power system connectivity monitoring using a graph theory network flow algorithm. *International Journal of Electrical Power & Energy Systems*, 78, 499–507.
- [10] Xu, B., Zhang, J., and Xu, L. (2021). A survey on graph theory applications in modern power systems. *CSEE Journal of Power and Energy Systems*, 7(4), 945–960.
- [11] Zhang, X., Liu, H., and Huang, J. (2022). A novel fault diagnosis method for power grid based on graph theory. *Frontiers in Energy Research*, 10, 1020687.
- [12] Xu, R., Chen, X., and Zhou, Z. (2021). Graph neural networks for fault diagnosis in power systems: A review. *IEEE Transactions on Systems, Man, and Cybernetics: Systems*, 51(11), 6643–6656.
- [13] Singh, B., and Khaparde, S. A. (2019). Fault diagnosis in distribution networks using wavelet transforms and artificial intelligence. *Electric Power Systems Research*, 170, 229–237.
- [14] Chen, S., Wang, L., and Wu, Q. (2023). Transformer-based architectures for intelligent substation relay protection systems. *IEEE Transactions on Power Delivery*, 38(2), 845–856.
- [15] Jones, T., Smith, A., and Zhao, Y. (2023). Digital twin-enabled situational awareness in power distribution systems. *IEEE Transactions on Industrial Informatics*, 19(4), 2870–2879.
- [16] Smith, J., Brown, P., and Liao, F. (2020). Distributed fault diagnosis in microgrids using multi-agent systems. *IEEE Transactions on Smart Grid*, 11(3), 2129–2138.
- [17] Zhao, H., Li, B., and Song, H. (2019). BFS algorithm for fast fault path identification in smart grids. *Journal of Modern Power Systems and Clean Energy*, 7(4), 845–853.
- [18] Gao, Y., Li, K., and Wu, D. (2022). Application of knowledge graph in power system fault diagnosis and disposal. *Frontiers in Energy Research*, 10, 988280.
- [19] Khalid, M. U., and Guerrero, J. M. (2021). Adaptive protection coordination in microgrids: Current status and challenges. *Renewable Power Generation*, 15(6), 564–578.
- [20] Jones, M. T., and Brown, L. (2021). Event-driven architecture for substation automation. *Electric Power Systems Research*, 195, 107135.

- [21] Baran, M. E., and Wu, F. F. (1989). Network reconfiguration in distribution systems for loss reduction and load balancing. *IEEE Transactions on Power Delivery*, 4(2), 1401–1407.
- [22] Kersting, W. H. (2001). Radial distribution test feeders. *IEEE Transactions on Power Delivery*, 6(3), 975–985.
- [23] CIGRE Working Group C6.04.02. (2015). CIGRE OV study: Medium-voltage distribution network of the future. *Electra*, 269, 45–54.
- [24] Girgis, A. A., and El-Shanawany, M. (1995). A fault-analysis-based approach for protection of distribution systems with distributed generation. *IEEE Transactions on Power Delivery*, 10(1), 379–384.
- [25] Zhao, L., and Dong, Z. Y. (2013). A review of microgrid protection and control techniques. *CSEE Journal of Power and Energy Systems*, 1(3), 22–31.

Biographies

Li Kaiyun, a native of Fengqing, Yunnan Province, studied at the School of Electrical Engineering of Kunming University of Science and Technology from 2013 to 2017 and obtained a bachelor's degree. I have been working at Lincang Power Supply Bureau of Yunnan Power Grid Co., Ltd. since August 2017, and have been working in the substation repair and testing Institute for 8 years. As a team member, team leader and deputy manager, I have successively participated in and completed multiple large-scale projects such as the 500kV Boshang integrated automation transformation, series compensation transformation, and the construction of the 220kV Fengshan intelligent Station, and have also taken on the review work of many projects.

Wang Xiqiong, a native of Xiangyun, Yunnan Province, studied at the School of Electrical and Information Engineering of Southwest Minzu University from 2012 to 2016 and obtained a bachelor's degree. I have been working at Lincang Power Supply Bureau of Yunnan Power Grid Co., Ltd. since July 2016, and have been working in the substation repair and testing Institute for 9 years. Senior secondary on-site operation and maintenance worker, has successively participated in and completed multiple large-scale projects such as the infrastructure project of 220kV Dengke Substation, regular inspection of 500kV Boshang Substation, and construction of Baoxin sub-station of 35kV substation, and has also undertaken the review work of many projects.

Chen Wei, a native of Meishan, Sichuan Province, studied at Chongqing Electric Power College from 2006 to 2009. In July 2009, he joined Lincang Power Supply Bureau of Yunnan Power Grid Co., Ltd. and has been working there ever since. He has been working in the substation repair and testing Institute for 16 years. As a team member and team leader, I have successively participated in and completed multiple large-scale projects such as the 500kV Boshang integrated automation transformation, the series compensation transformation, and the construction of the 220kV Dengke substation, and have also taken on the review work of many projects.

Zeng Kaizhi, a native of Fengqing, Yunnan Province, studied at the School of Electrical Engineering of Kunming University of Science and Technology from 2015 to 2019 and obtained a bachelor's degree. I have been working at Lincang Power Supply Bureau of Yunnan Power Grid Co., Ltd. since June 2019. I have been working in the Substation Repair and Testing Institute for six years. As a team member and deputy team leader, I have successively participated in and completed multiple large-scale projects, including the construction of 220kV Xiben Substation, the integrated automation transformation of 500kV Boshang Substation, the intelligent station construction of 220kV Fengshan Substation, the series compensation transformation of 500kV, and the installation of 500kV new energy control sub-stations. I have also taken on the review work of many projects.